Soil Moisture Estimation under Vegetation applying Polarimetric Decomposition Techniques

Thomas Jagdhuber, Helmut Schön, Irena Hajnsek, Konstantinos P. Papathanassiou

Microwave and Radar Institute, German Aerospace Center (DLR),
PO BOX 1116, 82234 Wessling, Germany,
Phone/Fax: +49-8153-28-2329 / -1449
Email: Thomas.Jagdhuber@dlr.de, Helmut.Schoen@dlr.de
Irena.Hajnsek@dlr.de, Kostas.Papathanassiou@dlr.de

ABSTRACT

Polarimetric decomposition techniques and inversion algorithms are developed and applied on the OPAQUE data set acquired in spring 2007 to investigate their potential and limitations for soil moisture estimation. A three component model-based decomposition is used together with an eigenvalue decomposition in a combined approach to invert for soil moisture over bare and vegetated soils at L-band.
The applied approach indicates a feasible capability to invert soil moisture after decomposing volume and ground scattering components over agricultural land surfaces. But there are still deficiencies in modeling the volume disturbance. The results show a root mean square error below 8.5vol.-% for the winter crop fields (winter wheat, winter triticale and winter barley) and below 11.5Vol-% for the summer crop field (summer barley) whereas all fields have a distinct volume layer of 55-85cm height.

1. INTRODUCTION

Soil moisture represents a key observable in flood forecasting and hydrological modeling. In order to identify critical catchment states before flooding events the possibility to retrieve soil moisture on a catchment scale from a SAR system with frequent coverage is highly desirable. Since most of the landscape in mid-Europe is at least seasonally covered by vegetation, the estimation of soil moisture increases in complexity due to the presence and gradual increase of vegetation over the growing season. In order to estimate soil moisture under the vegetation layer the volume needs to be subtracted. For this reason polarimetry is used to increase the amount of observables.
The main goal is to investigate the potential of polarimetric decomposition techniques to separate the individual scattering contributions within one resolution cell. A combination of an eigenvalue and a model-based decomposition is applied on L-band data to invert soil moisture. In the following the polarimetric decomposition techniques, the application on experimental data including inversion and validation for four different crop types are presented.

2. POLARIMETRIC DECOMPOSITION TECHNIQUES

Fig. 1 represents a scheme for application of the polarimetric decomposition techniques and inversion algorithms for soil moisture estimation. In a first step an eigenvalue decomposition is applied to calculate the polarimetric entropy (H) and alpha (α) values [1]. An H/α-criterion is calculated from the X-Bragg model of [2] considering the incidence angle and a maximum soil moisture of 50vol.-% to determine the limiting entropy and alpha values for surface scattering. Pixels matching this criterion are classified as non-vegetated bare soil pixels and are inverted for soil moisture via the X-Bragg inversion approach published in [2].

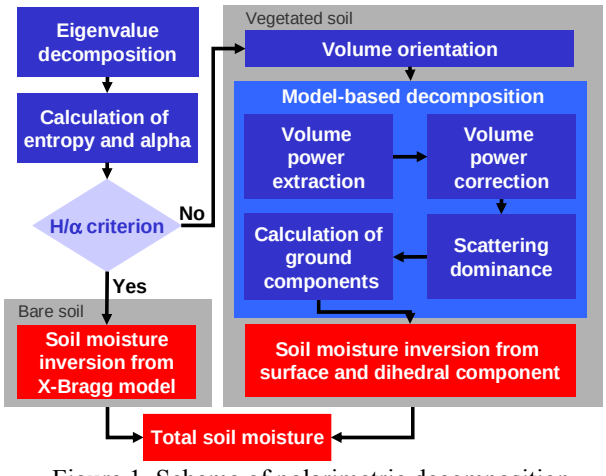

Figure 1. Scheme of polarimetric decomposition techniques and inversion algorithms for soil moisture

For pixels not matching the criterion a scattering scenario consisting of ground and vegetation components is assumed. In order to select the orientation of a vegetation volume the approach of Yamaguchi et al. [3] is applied to model the

$$\langle [T_{tot}] \rangle = \langle [T_{XB}] \rangle + \langle [T_{AD}] \rangle + \langle [T_V] \rangle$$

$$\langle [T_{tot}] \rangle = f_s \begin{bmatrix} 1 & \beta^* \operatorname{sinc}(2\psi) & 0 \\ \beta \operatorname{sinc}(2\psi) & 0.5 \cdot |\beta|^2 (1 + \operatorname{sinc}(4\psi)) & 0 \\ 0 & 0 & 0.5 \cdot |\beta|^2 (1 - \operatorname{sinc}(4\psi)) \end{bmatrix} + f_d \cdot L_s \cdot L_v \begin{bmatrix} |\alpha|^2 & \alpha & 0 \\ \alpha^* & 1 & 0 \\ 0 & 0 & 0 \end{bmatrix} + f_v \begin{bmatrix} C_1 & C_4 & 0 \\ C_4 & C_2 & 0 \\ 0 & 0 & C_3 \end{bmatrix} \tag{1}$$

vegetation layer with horizontally oriented, vertically oriented or randomly oriented dipoles. After the estimation of the volume orientation, the volume power f_v is extracted by solving Eq. 1 using the respective volume. As the three component decomposition can lead to negative eigenvalues of the ground components, the volume power f_v is corrected for the different volume orientation cases according to [4]. After the subtraction of the corrected and selected volume component the ground components are used to estimate the scattering dominance by a criterion defined in [5] to set the parameter α or β in the non-dominant case to zero [6].
Subsequently either the dihedral or the surface component is inverted for soil moisture depending on the scattering dominance. As a last step the estimated soil moistures from the bare soil and the vegetated soil areas are unified in one total soil moisture result. A more detailed description of the single methods is given below.

A. Method for bare soil

The extended Bragg model (X-Bragg) of [2] results in the coherency matrix $[T_{XB}]$ shown in Eq. 2 consisting of a term ψ controlling the depolarization as well as the

$$\langle [T_{XB}] \rangle = f_s \begin{bmatrix} 1 & \beta^* \operatorname{sinc}(2\psi) & 0 \\ \beta \operatorname{sinc}(2\psi) & 0.5 \cdot |\beta|^2 (1 + \operatorname{sinc}(4\psi)) & 0 \\ 0 & 0 & 0.5 \cdot |\beta|^2 (1 - \operatorname{sinc}(4\psi)) \end{bmatrix} \tag{2}$$

level of roughness and the parameters f_s and β

$$f_s = \frac{m_s^2}{2} |R_h + R_v|^2 \qquad \beta = \frac{R_h - R_v}{R_h + R_v} \tag{3}$$

which are functions of the Bragg coefficients (R_h, R_v) and a roughness parameter m_s

$$R_h = \frac{\cos\theta - \sqrt{\varepsilon_s - \sin^2\theta}}{\cos\theta + \sqrt{\varepsilon_s - \sin^2\theta}} \tag{4}$$

$$R_v = \frac{(\varepsilon_s - 1)\left(\sin^2\theta - \varepsilon_s\left(1 + \sin^2\theta\right)\right)}{\left(\varepsilon_s \cos\theta + \sqrt{\varepsilon_s - \sin^2\theta}\right)^2} .$$

The Bragg coefficients depend on the dielectric constant of the soil ε_s and the incidence angle θ.
For the inversion the calculated entropy and alpha values from the data are compared with the entropy and alpha values of the X-Bragg model coherency matrix formed by a variety of ε_s-values and the according incidence angle in order to find the closest match and the desired dielectric constant value, that is converted into soil moisture by a universal polynomial [7].

B. Method for vegetated soil

Selection of the volume orientation
The orientation of the volume is estimated by a power ratio P_r [3].

$$P_r = 10 \cdot \log \frac{\left\langle |S_{VV}|^2 \right\rangle}{\left\langle |S_{HH}|^2 \right\rangle} \tag{5}$$

$P_r < -2dB$ - vertically oriented dipoles
$-2 < P_r < 2dB$ - randomly oriented dipoles
$P_r > 2dB$ - horizontally oriented dipoles

For modeling a randomly oriented volume of dipoles the orientation distribution results in a distribution width of $\Delta\tau = 2\pi$ and a probability density function (pdf) of $p(\tau) = 1/(2\pi)$ within $0 < \tau < 2\pi$. For modeling an oriented volume of dipoles the orientation distribution results in a distribution width of $\Delta\tau = \pi$. For vertical orientation the pdf as $p(\tau) = (1/2)\sin\tau$ is defined within $0 < \tau < \pi$, whereas for horizontal orientation the pdf as $p(\tau) = (1/2)\cos\tau$ within $-\pi/2 < \tau < \pi/2$ is used. Finally the following volume coherency matrices are derived:

General

$$\langle [T_V^g] \rangle = f_v \begin{bmatrix} C_1 & C_4 & 0 \\ C_4 & C_2 & 0 \\ 0 & 0 & C_3 \end{bmatrix}$$

Vertical

$$\langle [T_V^v] \rangle = \frac{f_v}{30} \begin{bmatrix} 15 & 5 & 0 \\ 5 & 7 & 0 \\ 0 & 0 & 8 \end{bmatrix} \tag{6}$$

Random

$$\langle [T_V^r] \rangle = \frac{f_v}{4} \begin{bmatrix} 2 & 0 & 0 \\ 0 & 1 & 0 \\ 0 & 0 & 1 \end{bmatrix}$$

Horizontal

$$\langle [T_V^h] \rangle = \frac{f_v}{30} \begin{bmatrix} 15 & -5 & 0 \\ -5 & 7 & 0 \\ 0 & 0 & 8 \end{bmatrix}$$

Volume power extraction
After retrieval of the appropriate volume matrix Eq. 1 is solved for the volume parameter f_v, whereas for ψ an empirical first estimate of $\pi/12$ is assumed. It is important to note that f_v is calculated differently

according the volume orientation and the scattering dominance. Since this is only known in a later step both f_v-values, from surface and from dihedral dominant cases, have to be calculated until the scattering dominance is determined.

Correction of volume power

A remaining coherency matrix [T_V^{rem}] is calculated as displayed in Eq. 7 and solved for its three eigenvalues [4]. The three eigenvalue equations are set to zero and solved for f_v.

$$\left\langle \left[T_V^{rem}\right] \right\rangle = \begin{bmatrix} T_{11} & T_{12} & 0 \\ T_{12}^{*} & T_{22} & 0 \\ 0 & 0 & T_{33} \end{bmatrix} - f_v \begin{bmatrix} C_1 & C_4 & 0 \\ C_4 & C_2 & 0 \\ 0 & 0 & C_3 \end{bmatrix} \quad (7)$$

These solutions for f_v are compared with the extracted f_v of the previously calculated three component decomposition to find the minimum f_v-value. This minimum f_v is used in the next step for the retrieval of the ground components (surface, dihedral).

Soil moisture inversion from ground components

In the next step the retrieved volume component [T_V] is subtracted from the ground components (surface [T_{XB}], dihedral [T_{AD}]) in order to retrieve the characteristics from the underlying soil. The surface component [T_{XB}] is modeled as an X-Bragg surface component according to Eqs. 2-4 and can be inverted into soil moisture via the ratio β [8, 9]. The dihedral component [T_{AD}] is modeled as a Fresnel reflection of the soil and the perpendicular stem of a plant with the parameters α and f_d

$$\alpha = \frac{R_{s,h}R_{t,h} - R_{s,v}R_{t,v}e^{i\varphi}}{R_{s,h}R_{t,h} + R_{s,v}R_{t,v}e^{i\varphi}} \quad (8)$$

$$f_d = \frac{1}{2}\left|R_{s,h}R_{t,h} + R_{s,v}R_{t,v}e^{i\varphi}\right|^2$$

which are functions of the Fresnel coefficients ($R_{s,v}$, $R_{s,h}$, $R_{t,v}$, $R_{t,h}$) and a phase difference φ depending on the incidence angle θ and the dielectric constant of the surface ε_s and of the trunk ε_t [9]. Additionally a vegetation attenuation term L_v and a roughness loss term L_s are introduced in order to account for the vegetation attenuation during the propagation through the vegetation layer as well as for the scattering loss caused by the soil roughness of the dihedral backscattering amplitude f_d:

$$L_v = \exp(-1/(\mu_{\max} - \mu_{\min})) \quad (9)$$

$$L_s = \exp(-2 \cdot ks^2 \cdot \cos^2\theta) \qquad ks = 1 - A \quad (10)$$

In Eq. 9 μ_{max} and μ_{min} represent the maximum and minimum ground to volume ratios, which can be calculated by the eigenvalues of the summed ground component matrices ([T_S]+[T_D]): $\mu_{max}=\lambda_1/P_v$ and $\mu_{min}=\lambda_2/P_v$. In Eq. 10 ks is the product of the vertical wave number k and the standard deviation of the vertical roughness s, which can be estimated from the anisotropy A as published in [2]. The dihedral component can be inverted to soil moisture via f_d and α after removal of the vegetation attenuation and the roughness loss [8, 9].

3. EXPERIMENTAL RESULTS

The decomposition and inversion algorithms were applied on the data set of the OPAQUE campaign, which was conducted in May 2007 by the University of Potsdam, the German Research Centre for Geoscience (GFZ) and the German Aerospace Center (DLR) in the Weißeritz catchment area near Dresden, Germany. The OPAQUE campaign studies operational discharge and flooding predictions in head catchments and aims to reduce the uncertainties in flood forecasting and prediction of rainfall-runoff processes by identifying critical catchment states caused by saturated soil layers [10]. In the frame of this campaign full-polarimetric SAR data (L-band) were acquired by the E-SAR sensor of DLR. Simultaneously, soil moisture was measured with time domain reflectrometry (TDR) probes by the University of Potsdam and GFZ on selected test fields with different vegetation and soil types. In addition, vegetation parameters were collected to characterize the biomass layer.

3.1. Polarimetric Decomposition

Focusing on the left image of Fig. 3 the result of the three component decomposition is shown in an RGB-image of the normalized power components, where the dihedral power is set to red, the volume power is set to green and the surface power is set to blue. Comparing the RGB-image with the land use map the forested areas show a clear and homogenous volume scattering signature, whereas on the agricultural fields surface or dihedral scattering are mainly dominant except for the winter rape fields which also illustrate a distinct volume scattering component, due to a dense vegetation layer of 120cm height. The image was taken in the end of May 2007 when most of the agricultural areas, especially the winter crops, were already covered by vegetation of at least 50cm height. Therefore the dihedral scattering is strongly visible, which can be seen on the winter triticale (which is a crossing of wheat and rye plants) and winter barley fields in the middle of the image.

Furthermore the bare soil fields show a clear surface dominance as expected.
But there are also fields which change their scattering dominance within the field parcel although the same crop type is present. One example is an area of grassland in the centre of the image, which changes in range direction from surface to dihedral scattering. This can be understood from Fig. 3, where the local incidence angle exhibits a clear gradient from steep angles of 25° to more shallow angles of 55°, which constitutes the influence of topography on the scattering dominance.

3.2. Soil moisture estimation

Fig. 4 displays the estimated soil moisture for the L-band scene of May 2007 for the single component X-Bragg approach, the surface and the dihedral component of the three component model-based decomposition. Additionally the sum of all soil moisture inversion approaches is presented in Fig. 4d. The inverted soil moisture values range from 0 to 50vol.-%, whereas the areas coloured in white represent non-invertible pixels. Starting with the soil moisture from the single component X-Bragg approach the areas classified for this approach are relatively sparse and lie mostly in the far range region. An exception are the black areas along azimuth direction which exhibit very steep incidence angles (< 5°) and cannot be considered any further. The level of inverted soil moisture values is quite high, which originates from the relatively low entropy and alpha values modeled with the X-Bragg model compared to the high entropy and alpha values from the data.
Soil moistures retrieved from the surface and dihedral scattering component of the three component decomposition show different densely inverted land use classes which are the result of the scattering dominance specified in the model-based decomposition. Hence, for the inversion from the surface component the summer corn fields on the lower right of the image, which were only sparsely vegetated at the time of acquisition, demonstrate a homogenous inversion result. The inversion from the dihedral component indicate a quite complete inversion for the winter triticale and the winter barley fields, which grew already to a vegetation height of more than 60cm causing a distinct dihedral scattering component. Finally Fig. 4d represents the sum of all inverted soil moistures, where major parts of the forested areas show a sparse inversion. In addition a long stretched region in near range illustrates a lack of inversion. This might be explained after comparison with the local incidence angle map within the regions of no inversion. Here the angles are below 20° incidence and the observable space spanned by polarimetry might limit the inversion.

4. VALIDATION

The four different crop types winter wheat, summer barley, winter triticale and winter barley were chosen for analysis of soil moisture estimation under vegetation cover. In order to describe the vegetation layer Tab. 1 and Fig. 2 are included.

Table 1. Description of vegetation volume for the investigated fields with different crop types

Vegetation parameters	Winter wheat	Summer barley	Winter triticale	Winter barley
Plant height [cm]	55	45	85	70
Row distance [cm]	10	23	10	10
Wet biomass [kg/m²]	2.85	0.93	3.34	3.31

The validation compares soil moisture values averaged from three ground measurement points in 0-5cm depth with the estimated soil moisture values from the surface and the dihedral scattering contribution in vol.-%. For the ground measurements TDR-probes of type "ThetaProbe ML2x" were used. For the retrieval of the estimated soil moistures a 9x9 box around the sampling points leading to 81 looks was taken for comparison regarding that only boxes with at least 10 invertible pixels were considered to avoid the influence of non-representative outliers. In Fig. 5 the correlation between measured and estimated soil moisture values for the four different crop types is displayed together with the root mean square error (RMSE) and the mean of the standard deviations (STDDEV) of the estimated soil moisture values (cf. Tab. 2).

Table 2. Root mean square error and mean of the standard deviations of estimated soil moisture values for the investigated fields

Fields	STDDEV	RMSE
Winter wheat	10.44	8.47
Summer barley	12.52	11.48
Winter triticale	10.61	8.45
Winter barley	12.31	8.50

The estimated soil moisture values on the winter wheat field show no significant trend and over- and underestimate the measured soil moisture. For the summer barley and the winter barley fields an underestimation is visible in Fig. 5 caused by the inverted soil moisture values of the surface component. This can be linked to a β-parameter that is too small after removal of the volume component. This leads to

the conclusion that the modeling of the vegetation volume is still not satisfactory. On the other hand soil moisture values from the triticale field are mostly inverted from the dihedral component and depict a slight overestimation, which might be induced by an overcompensation of the attenuation and roughness correction which is a first order estimate in order to keep the parameter space constant.

Figure 2. Photographs of investigated fields: Winter wheat (upper left), summer barley (lower left), winter triticale (upper right) and winter barley (lower right) on the day of acquisition (a scale bar is included showing the height of the vegetation.)

5. SUMMARY

Combined polarimetric decomposition techniques and inversion algorithms were applied on a L-band scene of the OPAQUE data set acquired by the E-SAR sensor of DLR. The single component X-Bragg approach can only be applied for a very limited amount of non-vegetated pixels and performs best in the shallow incidence region (>50°). The results of the three component model-based decomposition demonstrate its applicability on vegetated agricultural fields, as already denoted in [8].

Moreover, both ground scattering components (surface, dihedral) were used for the estimation of soil moisture under vegetation cover of at least 45cm height and 0.9kg/m² wet biomass. Finally the retrieved soil moisture values are validated against ground measurements taken with TDR probes. The RMSE of the estimated soil moistures from both scattering contributions (surface, dihedral) and from all investigated crop types exhibits an accuracy of 8.5-11.5vol.-%. Nevertheless a mean standard deviation of the estimated soil moistures of 10.4-12.3vol.-% indicates a broad range of inverted moisture values. Reasons for this might be on one side the complex and spatially highly varying scattering scenario inverted with a limited number of observables and on the other side the characteristics of soil moisture itself, which is also varying distinctly over one field parcel. Further investigations are necessary to gain a deeper understanding and to improve the modeling of the volume disturbance as well as studying the influence of topography on the inversion of soil moisture.

ACKNOWLEDGMENTS

The authors would like to thank the OPAQUE team (University of Potsdam and German Research Center for Geoscience (GFZ)) for their contribution to the field campaign and BMBF for supporting the activities.

REFERENCES

1. Cloude, S.R. & Pottier, E. (1996). A Review of Target Decomposition Theorems in Radar Polarimetry. IEEE Trans. Geosci. Remote Sensing, 34(2), 498-518.
2. Hajnsek, I., Pottier, E. & Cloude, S.R. (2003). Inversion of Surface Parameters From Polarimetric SAR. IEEE Trans. Geosci. Remote Sensing, 41(4), 727-744.
3. Yamaguchi,Y., Moriyama, T., Ishido, M. & Yamada, H. (2005). Four-Component Scattering Model for Polarimetric SAR Image Decomposition. IEEE Trans. Geosci. Remote Sensing, 43(8), 1699-1706.
4. van Zyl, J.J., Arii, M. & Ki, Y. (2008). Requirements for Model-Based Polarimetric Decompositions. Proc. 7th European Conference on Synthetic Aperture Radar (EUSAR), Friedrichshafen, Germany, 41-44.
5. Freeman, A. & Durden, S.L. (1998). A Three-Component Scattering Model for Polarimetric SAR Data. IEEE Trans. Geosci. Remote Sensing, 36(3), 963-973.
6. Yamaguchi, Y., Yajima, Y. & Yamada, H. (2006). A Four Component Decomposition of POLSAR Images Based on the Coherency Matrix. IEEE

Trans. Geosci. Remote Sensing Letters, 3(3), 292-296.
7. Topp, G.C., Davis, J.L. & Annan, A.P. (1980). Electromagnetic Determination of Soil Water Content: Measurements in Coaxial Transmission Lines. Water Resources Res., 16(3), 574-582.
8. Jagdhuber, T., Hajnsek, I., Schön, H. & Papathanassiou, K.P. (2008). Pol-SAR Time Series for Soil Moisture Estimation under Vegetation. Proc. 7th European Conference on Synthetic Aperture Radar (EUSAR), Friedrichshafen, Germany, 181-184.
9. Hajnsek, I., Jagdhuber, T., Schön, H. & Papathanassiou, K.P. Potential of Estimating Soil Moisture under Vegetation Cover by means of PolSAR. IEEE Trans. Geosci. Remote Sensing, in press.
10. Jagdhuber, T. & Hajnsek, I. (2009). OPAQUE 2007: Kampagnen- und Prozessierungsbericht. DLR-report, Oberpfaffenhofen, Germany

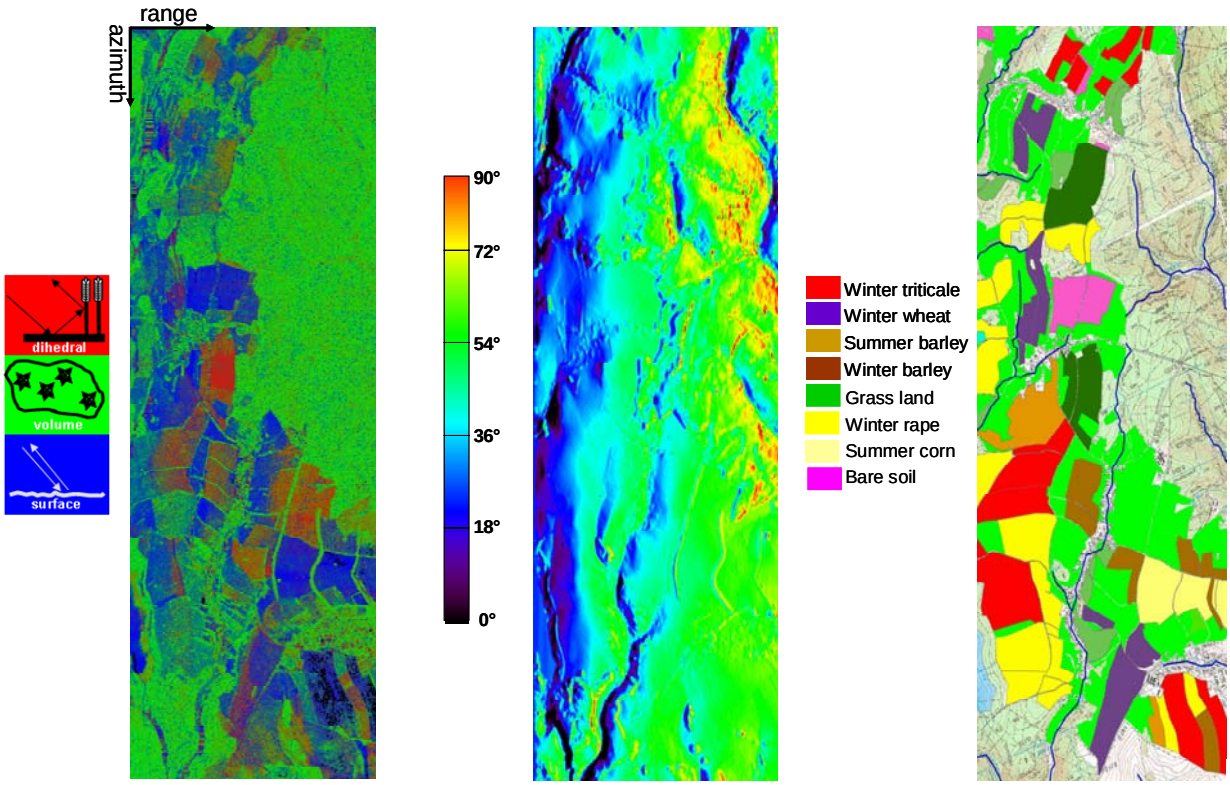

Figure 3. RGB-image of normalized power components after decomposition (R: Dihedral G: Volume B: Surface, black areas are inverted with X-Bragg method) (left), local incidence angle (middle) and land use (right) for the L-band scene.

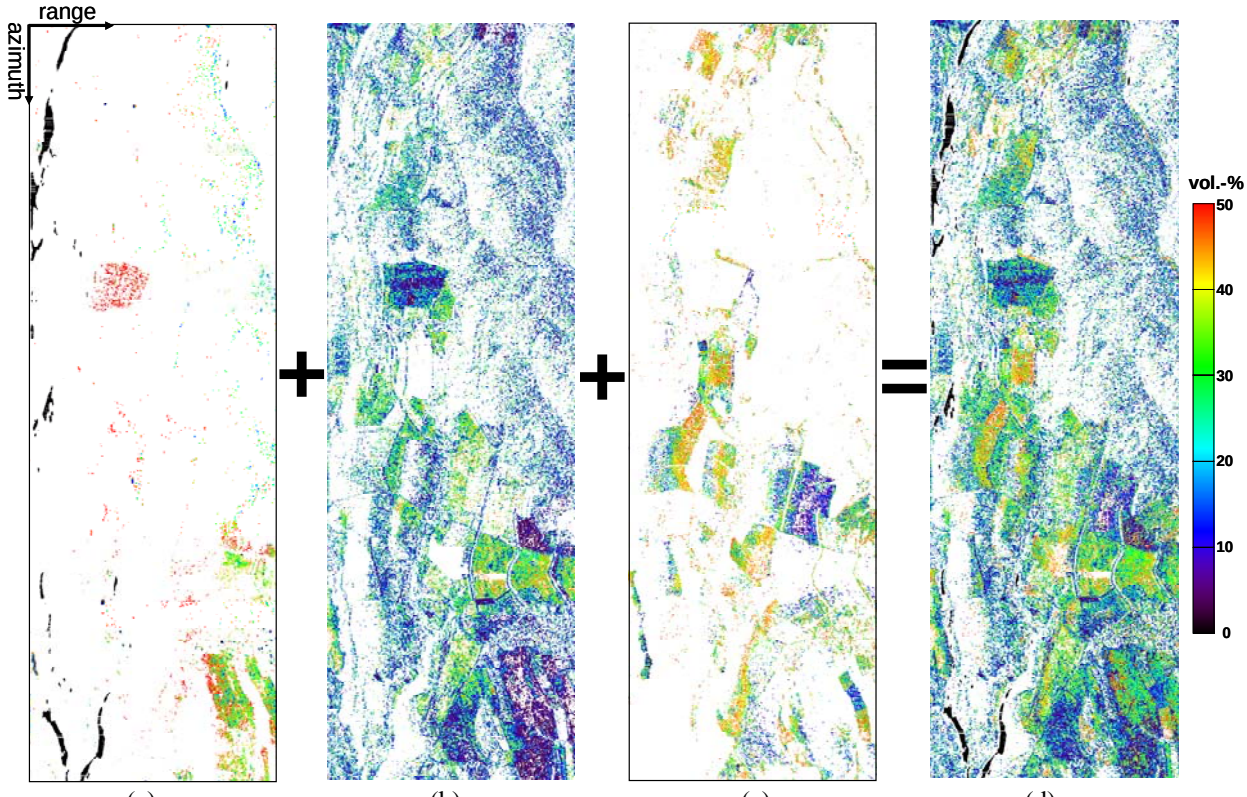

(a) (b) (c) (d)

Figure 4. Estimated soil moisture of (a) the single component X-Bragg method, (b) the surface and (c) the dihedral component of the three component model-based decomposition. (d) shows the total soil moisture. White colour represents non-invertible pixels (averaging window: 4x4).

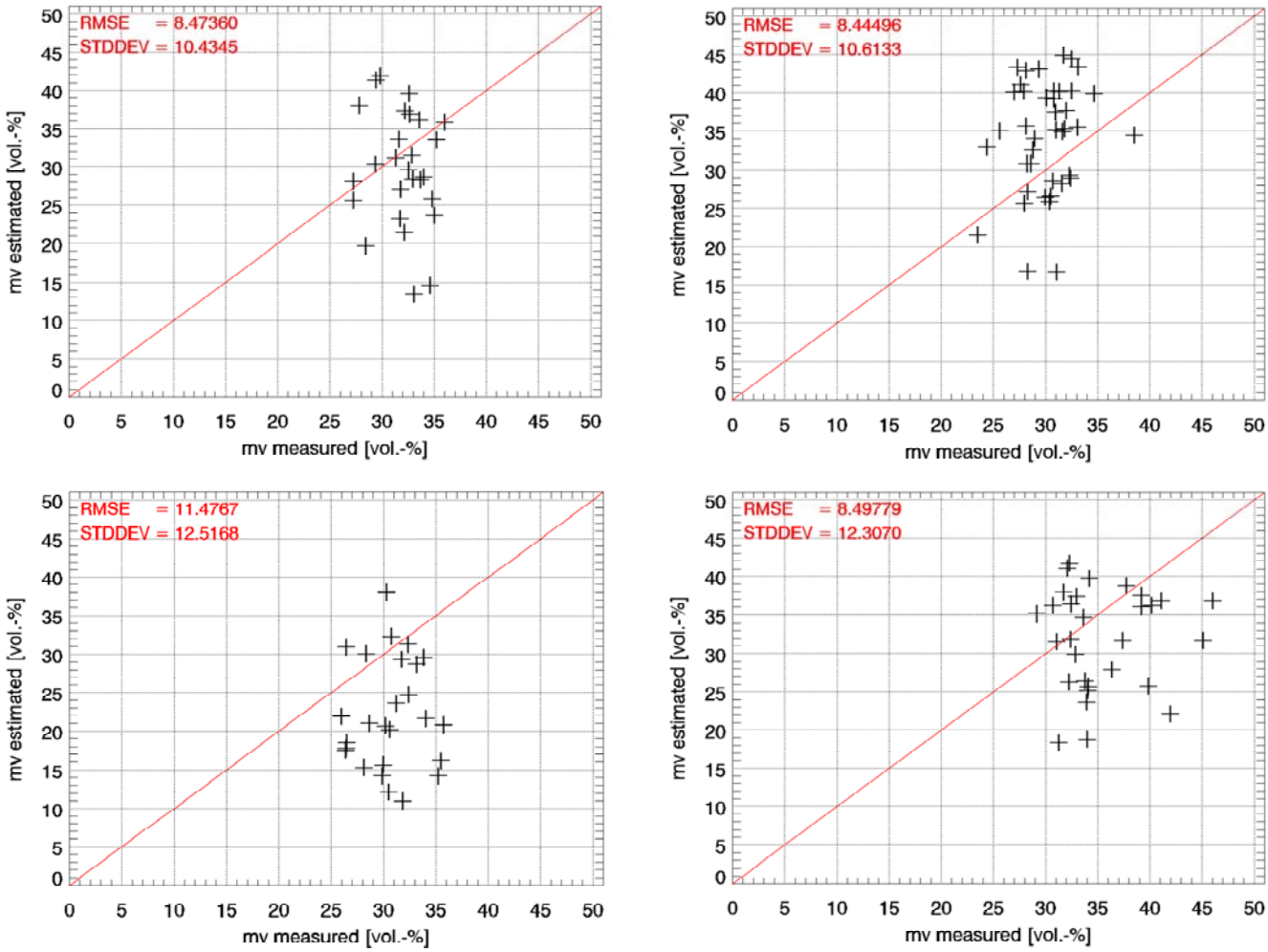

Figure 5. Correlation between measured and estimated soil moisture values in vol.-% for winter wheat (upper left), summer barley (lower left), winter triticale (upper right) and winter barley (lower right), RMSE = root mean square error of estimated soil moistures, STDDEV = mean of the standard deviations of estimated soil moistures.